Supporting Information

C_2/C_3 HYDROCARBON SEPARATION BY PRESSURE SWING ADSORPTION ON MIL-100(FE)

Vanessa F. D. Martins[1], Rute Seabra[1], Paulo Silva[1], Ana M. Ribeiro[1], Kyung Ho Cho[2], U-Hwang Lee[2], Jong-San Chang[2,3,*], José M. Loureiro[1], Alírio E. Rodrigues[1], Alexandre Ferreira[1,*]

[1] Laboratory of Separation and Reaction Engineering - Laboratory of Catalysis and Materials (LSRE-LCM),
Department of Chemical Engineering, University of Porto,
Rua Dr. Roberto Frias, s/n, 4200-465 Porto, Portugal.

[2] Catalysis Center for Molecular Engineering,
Korea Research Institute of Chemical Technology (KRICT),
141 Gajeong-ro, Jang-dong, Yuseong, Daejeon 34114, Republic of Korea

[3] Department of Chemistry,
Sungkyunkwan University,
Suwon 440-476, Seoul, Republic of Korea

*To whom correspondence should be adressed: Phone + 351 22 041 4835;
Fax: + 351 22 508 1674. E-mail: Alexandre Ferreira - aferreir@fe.up.pt, Jong-San Chang - jschang@krict.re.kr

Tables

Table S1. Main physical properties of MIL-100(Fe) sample in granule form.

Property	Granules
BET Surface area ($m^2 \cdot g^{-1}$)	1568
Micropore area ($m^2 \cdot g^{-1}$)	1457
External Surface area ($m^2 \cdot g^{-1}$)	110.9
Micropore volume ($cm^3 \cdot g^{-1}$)	0.58

Table S2. Experimental conditions of breakthrough curves performed at 323 K and 150 kPa.

Run	Step	Feed composition	Q_{Feed} (SLPM)	Bed initial state
Single Component				
1	Adsorption	C_2H_6	0.5	Filled with He
	Desorption	He	0.5	Filled with C_2H_6
2	Adsorption	C_2H_4	0.5	Filled with He
	Desorption	He	0.5	Filled with C_2H_4
3	Adsorption	C_3H_8	0.5	Filled with He
	Desorption	He	0.5	Filled with C_3H_8
Binary				
4	Adsorption	$0.30C_2H_6/0.70C_3H_8$	0.15/0.35	Filled with He
	Desorption	He	0.5	Filled with $0.30C_2H_6/0.70C_3H_8$
5	Adsorption	$0.30C_2H_4/0.70C_3H_8$	0.15/0.35	Filled with He
	Desorption	He	0.5	Filled with $0.30C_2H_4/0.70C_3H_8$
Pseudo-Binary				
6	Adsorption	C_2H_6	0.5	Filled with C_3H_8
	Desorption	C_3H_8	0.5	Filled with C_2H_6
7	Adsorption	C_2H_4	0.5	Filled with C_3H_8
	Desorption	C_3H_8	0.5	Filled with C_2H_4

Table S3. Experimental conditions for the VPSA cycles performed at 323 K.

Step	Counter-current pressurization	Adsorption	Rinse	Counter-current blowdown	Purge
Cycle scheme 1					
Time, s	235	480	300	300	100
Pressure, kPa	150	150	150	10	10
Feed, SLPM	0.6 (C_2H_6)	0.18/0.42 (C_2H_6/ C_3H_8)	0.6 (C_3H_8)	----------	0.15 (C_2H_6)
Bed initial state	Filled with C_2H_6 at 150 kPa				
Cycle scheme 2					
Time, s	235	480	300	300	150
Pressure, kPa	150	150	150	10	10
Feed, SLPM	0.6 (C_2H_4)	0.18/0.42 (C_2H_4/ C_3H_8)	0.6 (C_3H_8)	----------	0.15 (C_2H_4)
Bed initial state	Filled with C_2H_4 at 150 kPa				

Table S4. Henry's law constants for MIL-100(Fe) granules at three different temperatures.

Adsorbate	Henry constants, K_H (mol kg^{-1} kPa^{-1})			$-\Delta H_o$ (kJ mol^{-1})	K_{Ho} (mol kg^{-1} kPa^{-1})
	323 K	373 K	423 K		
Ethane	9.87×10^{-3}	3.85×10^{-3}	2.03×10^{-3}	18.02	1.19×10^{-5}
Ethylene	9.40×10^{-3}	4.50×10^{-3}	2.24×10^{-3}	16.23	2.29×10^{-5}
Propane	3.50×10^{-2}	1.09×10^{-2}	4.19×10^{-3}	24.09	4.51×10^{-6}

Table S5. Working capacities and selectivity parameters for MIL-100(Fe) granules at three different temperatures and different regeneration pressures.

	323 K (150 - 10 kPa)			373 K (150 - 10 kPa)			423 K (150 - 10 kPa)		
C_3/C_2 pair	$\Delta q_i/\Delta q_j$	K_{Hi}/K_{Hj}	$S_{i/j}$	$\Delta q_i/\Delta q_j$	K_{Hi}/K_{Hj}	$S_{i/j}$	$\Delta q_i/\Delta q_j$	K_{Hi}/K_{Hj}	$S_{i/j}$
Propane/Ethane (0.70/0.30)	6.6	3.5	23.3	7.7	2.8	21.6	7.2	2.1	14.9
Propane/Ethylene (0.70/0.30)	7.5	3.7	28.0	8.8	2.4	21.3	8.2	1.9	15.3
	323 K (150 - 50 kPa)			373 K (150 - 50 kPa)			423 K (150 - 50 kPa)		
Propane/Ethane (0.70/0.30)	4.0	3.5	14.2	5.2	2.8	14.7	5.1	2.1	10.4
Propane/Ethylene (0.70/0.30)	4.6	3.7	17.1	6.0	2.4	14.5	5.7	1.9	10.7

Table S6. Transport parameters.

Parameter	**Values**
Overall heat transfer coefficient (U), $W \cdot m^{-2} \cdot K^{-1}$	20
Film (gas-wall) heat transfer coefficient (h_w), $W \cdot m^{-2} \cdot K^{-1}$	45
Film (gas-particle) heat transfer coefficient (h_f), $W \cdot m^{-2} \cdot K^{-1}$	40
Heat axial dispersion coefficient (λ), $W \cdot m^{-1} \cdot K^{-1}$	0.3
Film mass transfer coefficient (k_f), m·s-1	2×10^{-2}
Axial dispersion coefficient (D_{ax}), $m^2 \cdot s^{-1}$	5×10^{-4}
Wall specific heat at constant pressure (C_{pw}), $J \cdot kg^{-1} \cdot K^{-1}$	500
Particle specific heat at constant pressure (C_{ps}), $J \cdot kg^{-1} \cdot K^{-1}$	1456
Crystal diffusivity on site A (D_{cA}), $m^2 \cdot s^{-1}$	C_2H_6: 4.7×10^{-09} C_2H_4: 1.1×10^{-08} C_3H_8: 1.6×10^{-09}
Crystal diffusivity on site B (D_{cB}), $m^2 \cdot s^{-1}$	C_2H_6: 1.8×10^{-09} C_2H_4: 2.7×10^{-09} C_3H_8: 7.7×10^{-09}

Table S7. VPSA performance parameters comparison between the results obtained for the cycles designed with those obtained for the same cycles, but considering (b_∞ a q_{sat}) by ±5%.

Cycle Scheme	Pu_R, %	Rec_R, %	$Prod_R$, *	Pu_X,%	Rec_X, %	$Prod_X$, *
	C_2H_6 or C_2H_4			C_3H_8		
1	**99.5**	**86.7**	**1.7**	**97.0**	**99.4**	**4.5**
1: q_{sat} - 5%	97.6	86.6	1.7	97.9	96.8	4.3
1: q_{sat} + 5%	99.9	79.7	1.5	95.5	99.9	4.5
1: b_∞ - 5%	98.8	85.8	1.7	97.6	98.4	4.4
1: b_∞ + 5%	99.8	83.4	1.6	96.3	99.8	4.5
2	**100.0**	**75.8**	**1.4**	**94.7**	**100.0**	**4.3**
2: q_{sat} - 5%	99.3	78.7	1.5	95.9	99.1	4.3
2: q_{sat} + 5%	100.0	68.9	1.3	93.3	100.0	4.3
2: b_∞ - 5%	99.8	76.9	1.4	95.4	99.7	4.3
2: b_∞ + 5%	100.0	72.2	1.3	93.9	100.0	4.3

Porosimetry by Hg intrusion

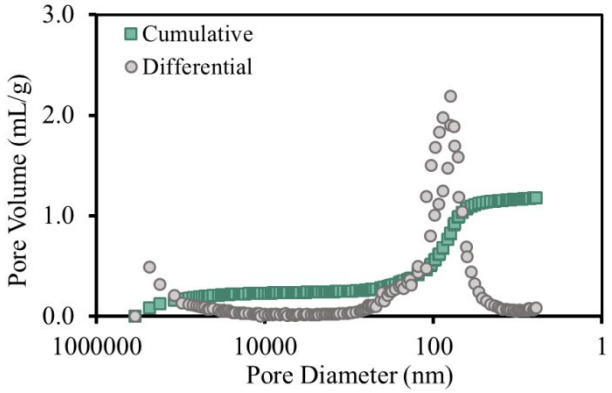

Figure S1. Inter-crystalline macropore size distribution by mercury intrusion of MIL-100(Fe) granules.

Isotherm Equilibrium Data

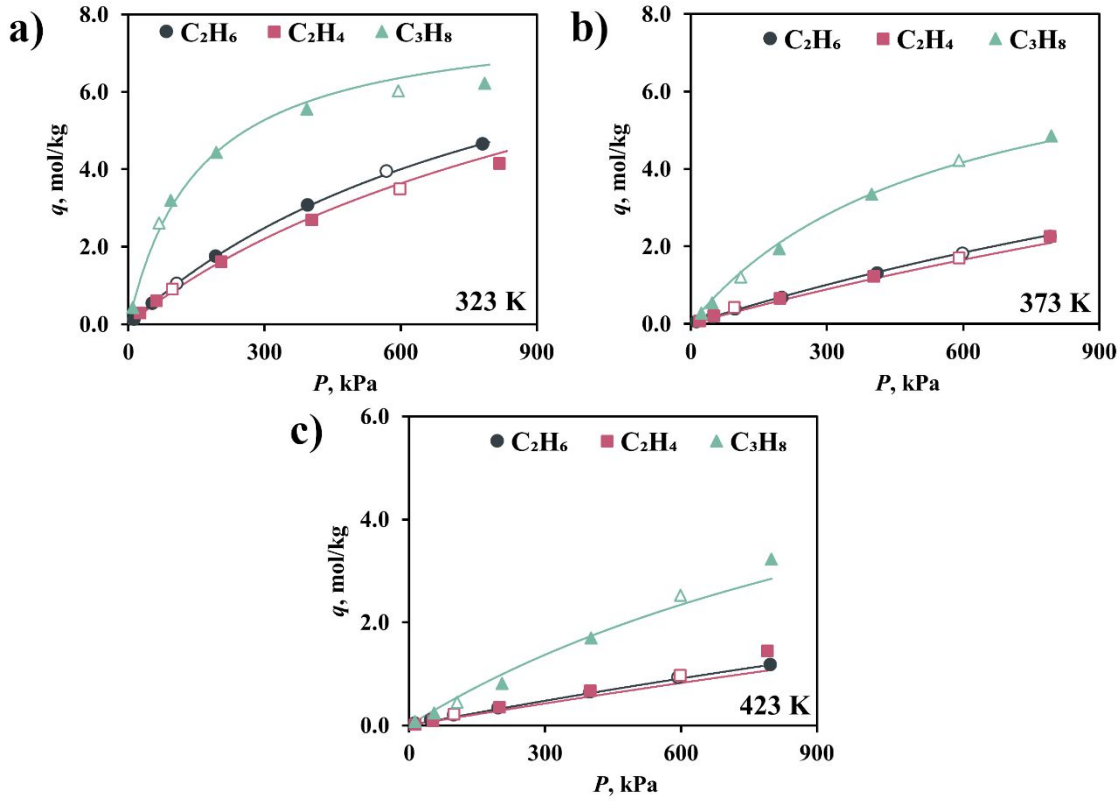

Figure S2. Adsorption isotherms measured on MIL-100(Fe) granules. Closed and open symbols represent adsorption and desorption branches, respectively and the lines correspond to the fitted DSL model.

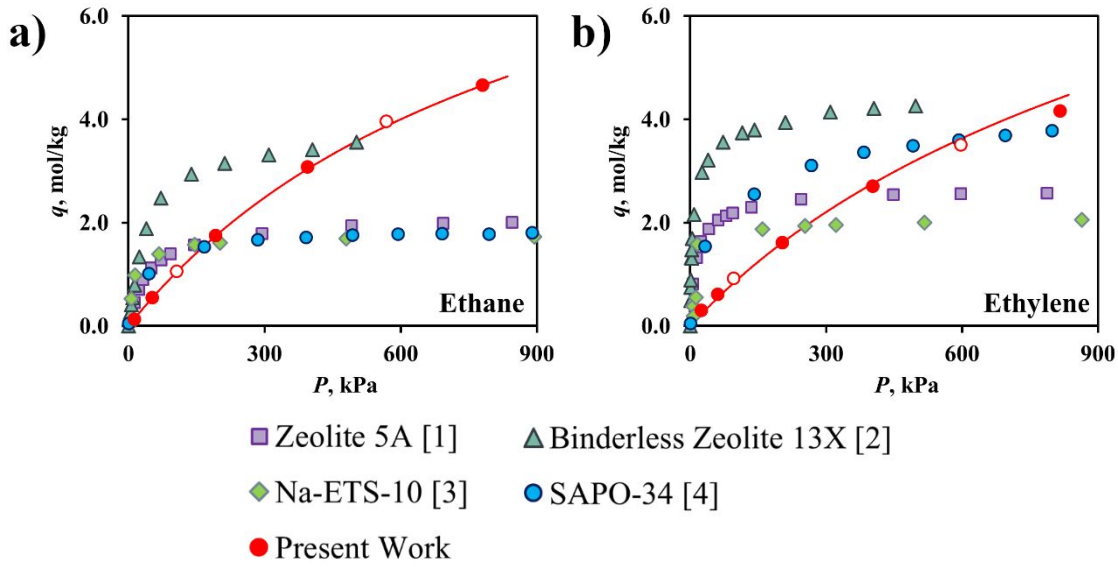

Figure S3. Adsorption isotherms comparison at 323 K, on different materials for: (a) ethane, and (b) ethylene [1-4].

Selectivity

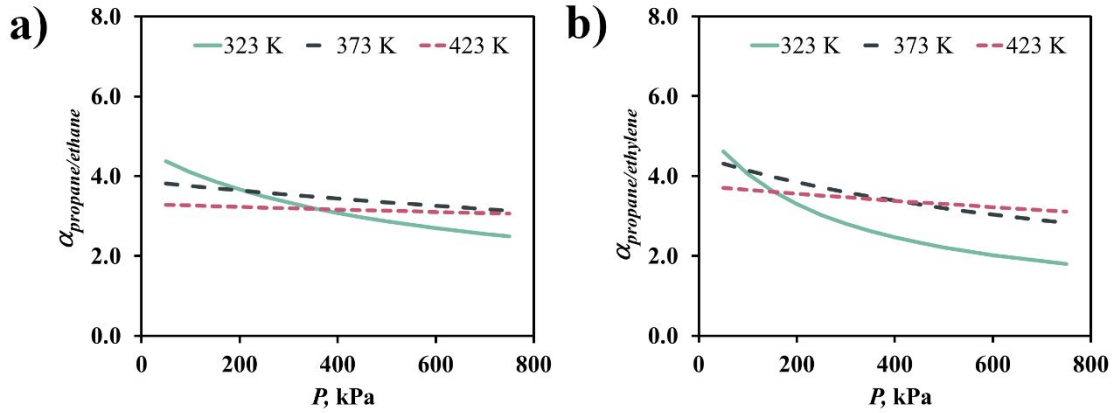

Figure S4. C_2/C_3 mixtures selectivity on MIL-100(Fe) granules as a function of the total pressure at 323, 373, and 423 K predicted by the ExDSL model: (a) 0.30/0.70 ethane/propane mixture, and (b) 0.30/0.70 ethylene/propane mixture.

Multicomponent adsorption equilibrium models

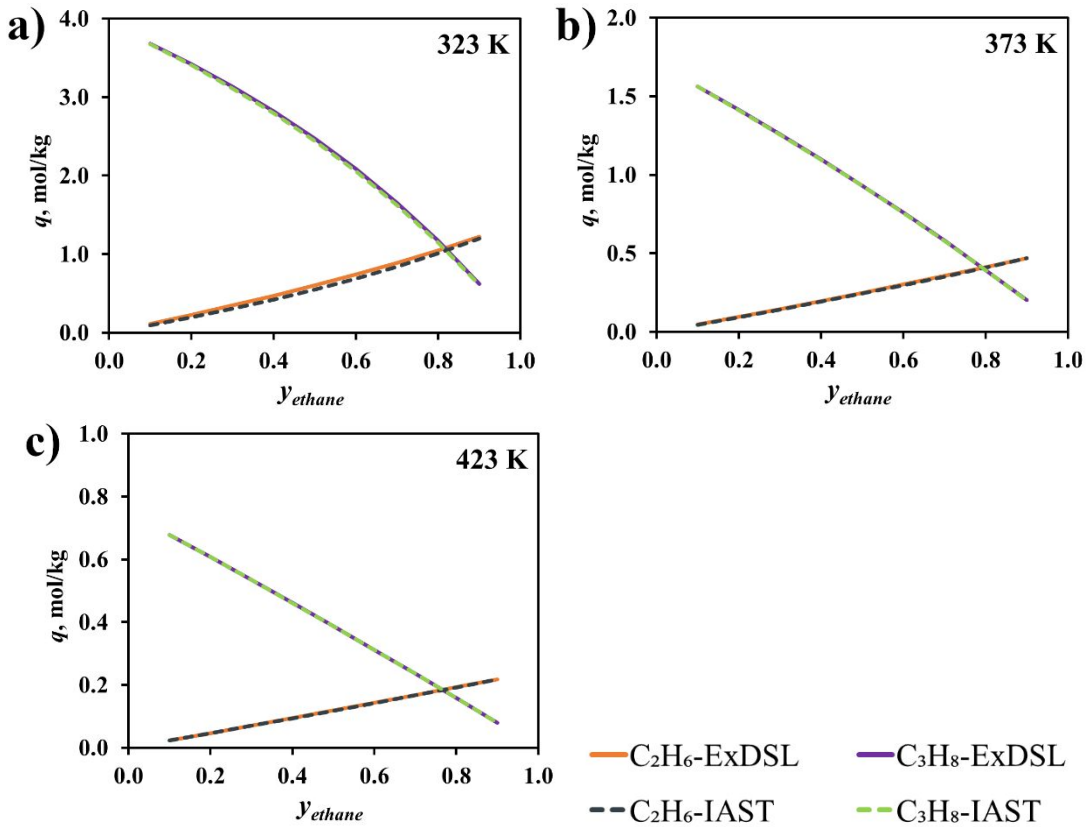

Figure S5. Binary ethane/propane adsorption equilibrium estimated by the ExDSL model and by the IAS theory as a function of the gas phase ethane molar fraction at 150 kPa, and at (a) 323, (b) 373, and (c) 423 K.

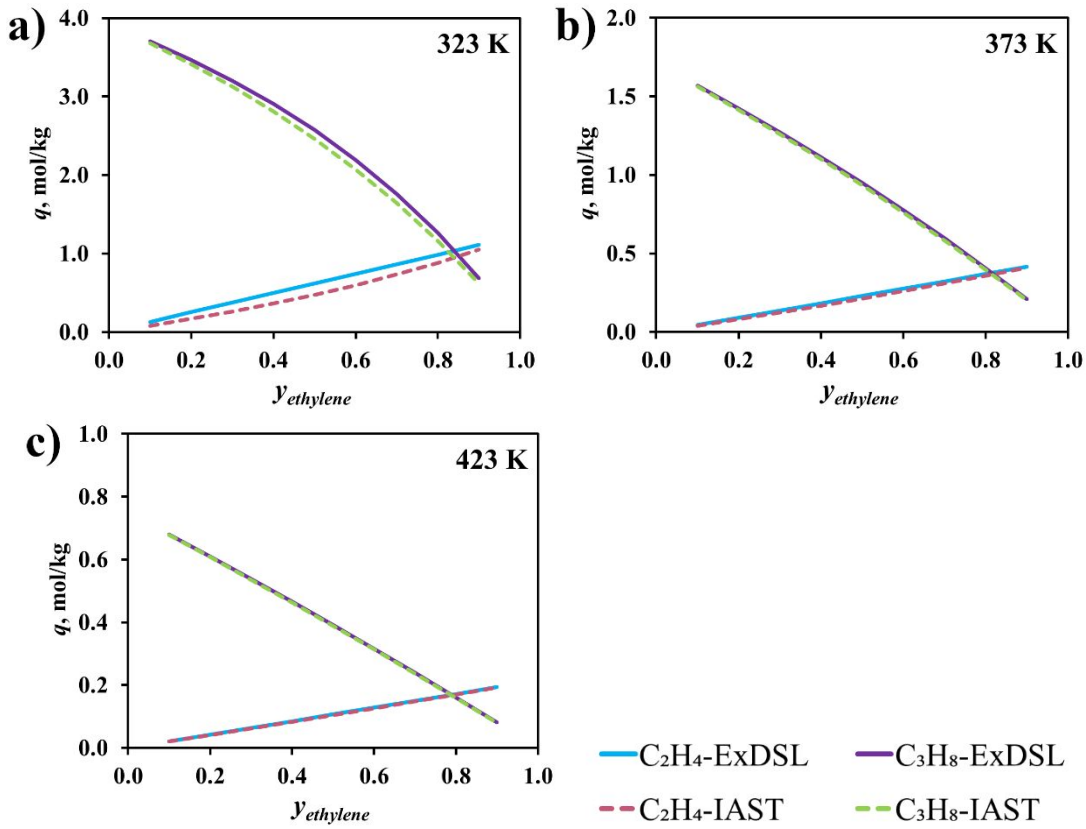

Figure S6. Binary ethylene/propane adsorption equilibrium estimated by the ExDSL model and by the IAS theory as a function of the gas phase ethylene molar fraction at 150 kPa, and at (a) 323, (b) 373, and (c) 423 K.

Transport Parameters:

To obtain the transport parameters included in the model it was necessary to estimate general properties of the gases and gas mixtures, like density, viscosity, molar specific heat and thermal conductivity. Viscosity of the pure components was obtained by the method of Chung et al. and the viscosity of the gas mixtures was calculated from the method of Wilke [5]. The thermal conductivities of the pure gases and gas mixtures were determined by the use of Eucken and Wassiljewa equations, respectively [5,6]. The transport parameters such molecular diffusivity and macropore diffusivity were estimated by the Chapman-Enskog and Bosanquet equations, respectively [6]. The values calculated for the micropore diffusivity according to the previously mentioned correlations are summarized in Table S4. The Wakao and Funazkri correlation was used to obtain the axial mass and heat dispersion coefficients [6]. The film heat transfer coefficient between the gas and the column wall was calculated with the Wasch and Froment correlation [6]. The only parameters that were adjusted to the experimental results were U and h_w, adjusted by the breakthrough experiments and then used in the simulations of the PSA cycles. The transport parameters obtained are summarized in Table S4.

Breakthrough curves

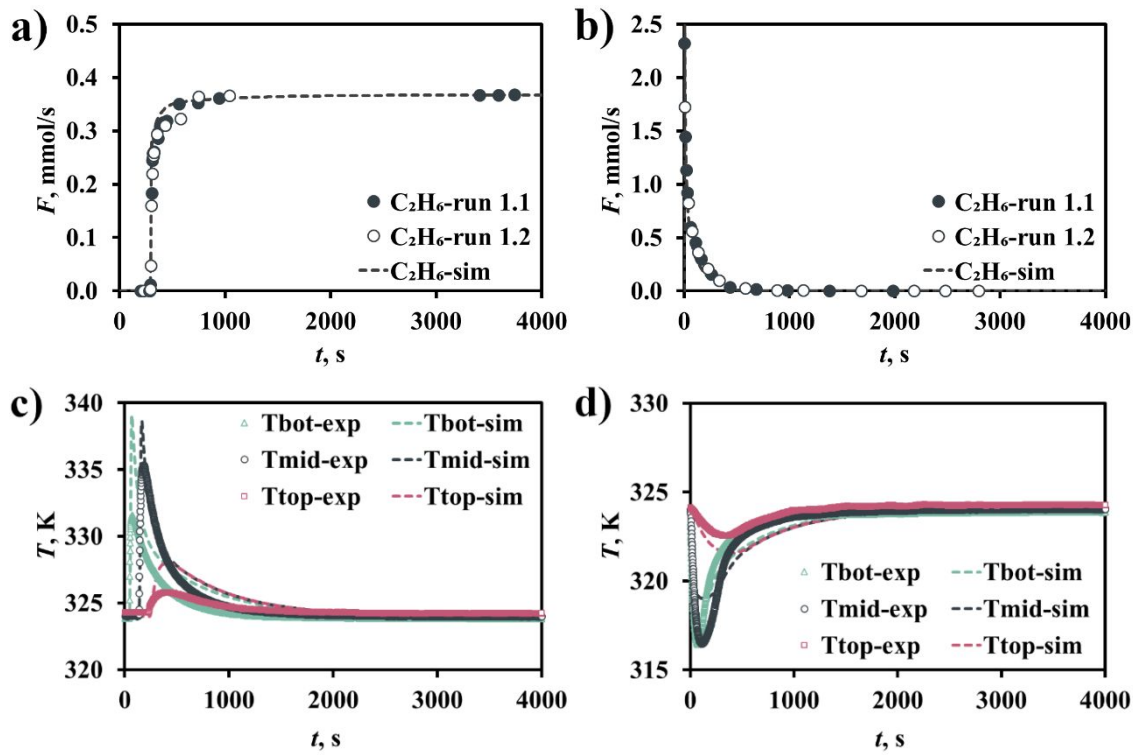

Figure S7. Molar flow rates (a) adsorption of ethane over a bed initially full of helium at 323 K and 150 kPa; (b) desorption of previously adsorbed ethane in flowing helium at 323 K and 150 kPa; gas temperature history along the (c) adsorption and (d) desorption at 0.17 m, 0.42 m and 0.67 m from the bottom end of the column. Symbols represent experimental results and solid lines simulation results.

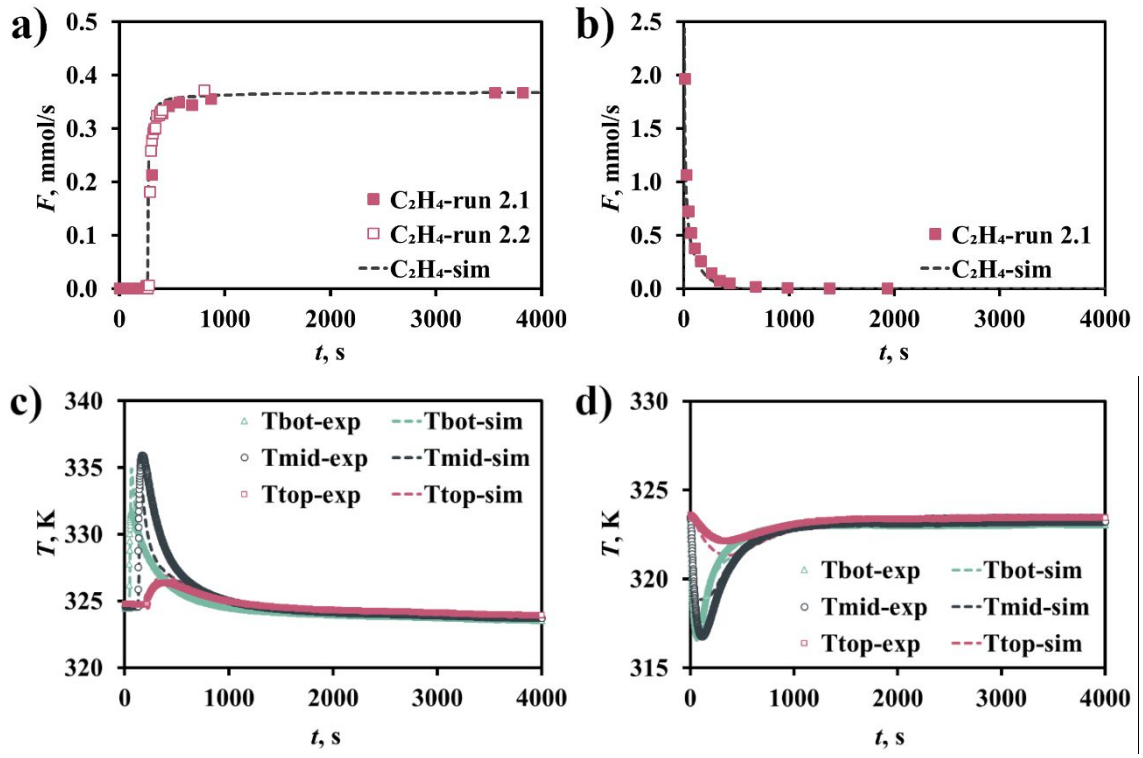

Figure S8. Molar flow rates (a) adsorption of ethylene over a bed initially full of helium at 323 K and 150 kPa; (b) desorption of previously adsorbed ethylene in flowing helium at 323 K and 150 kPa; gas temperature history along the (c) adsorption and (d) desorption at 0.17 m, 0.42 m and 0.67 m from the bottom end of the column. Symbols represent experimental results and solid lines simulation results.

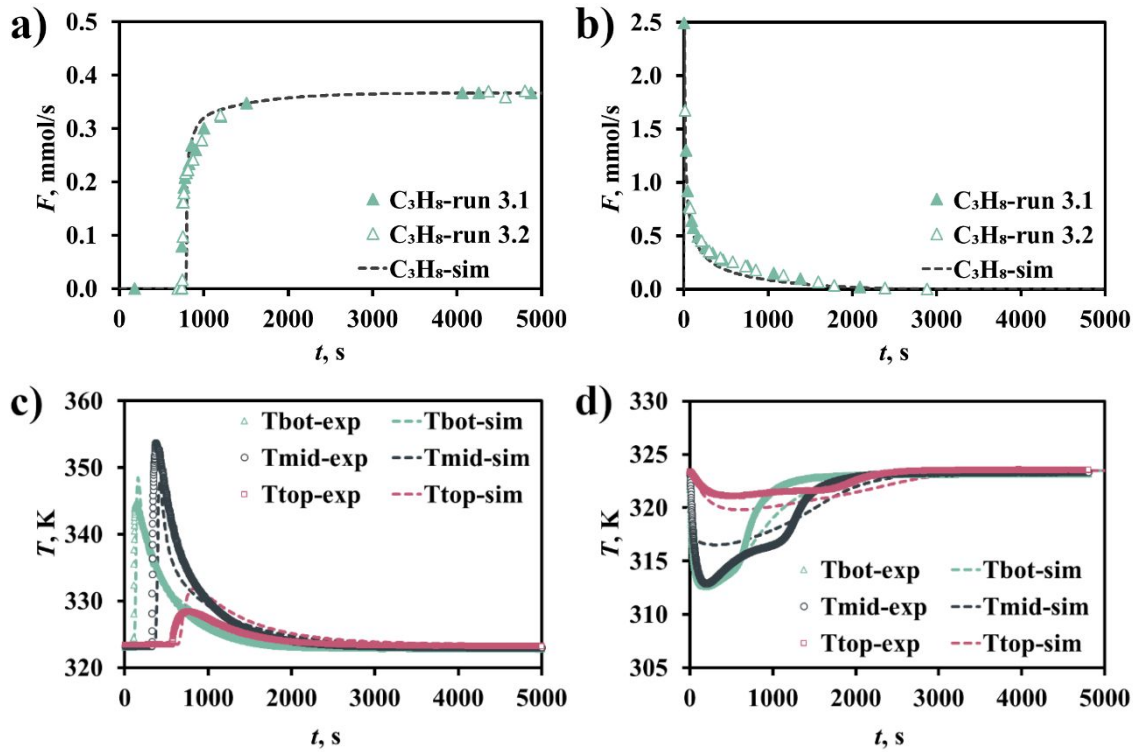

Figure S9. Molar flow rates (a) adsorption of propane over a bed initially full of helium at 323 K and 150 kPa; (b) desorption of previously adsorbed propane in flowing helium at 323 K and 150 kPa; gas temperature history along the (c) adsorption and (d) desorption at 0.17 m, 0.42 m and 0.67 m from the bottom end of the column. Symbols represent experimental results and solid lines simulation results.

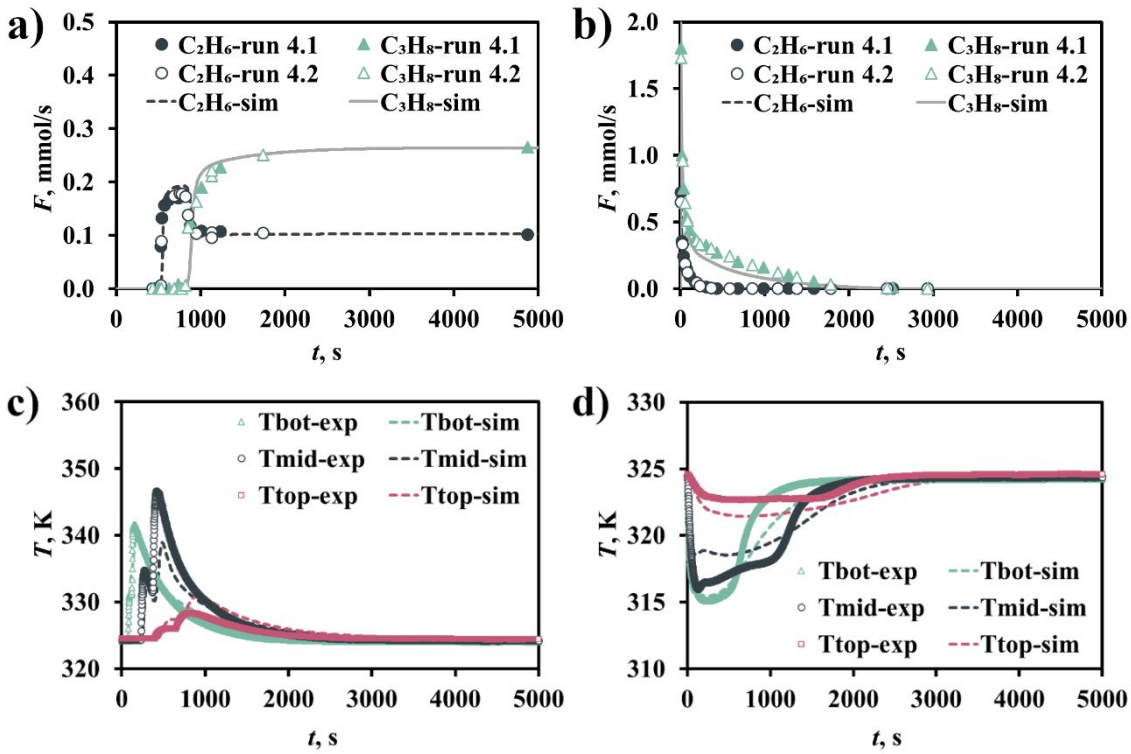

Figure S10. Molar flow rates (a) adsorption of a mixture 0.30/0.70 ethane/propane over a bed initially full of helium at 323 K and 150 kPa; (b) desorption of previously adsorbed mixture in flowing helium at 323 K and 150 kPa; gas temperature history along the (c) adsorption and (d) desorption at 0.17 m, 0.42 m and 0.67 m from the bottom end of the column. Symbols represent experimental results and solid lines simulation results.

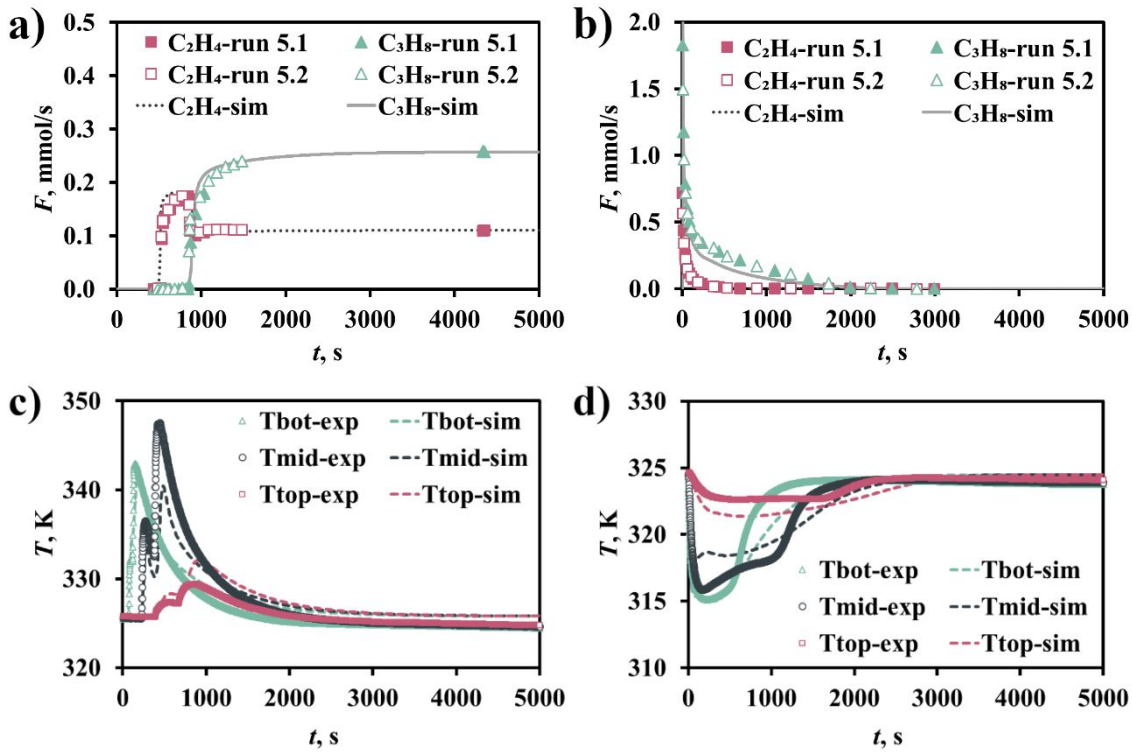

Figure S11. Molar flow rates (a) adsorption of a mixture 0.30/0.70 ethylene/propane over a bed initially full of helium at 323 K and 150 kPa; (b) desorption of previously adsorbed mixture in flowing helium at 323 K and 150 kPa; gas temperature history along the (c) adsorption and (d) desorption at 0.17 m, 0.42 m and 0.67 m from the bottom end of the column. Symbols represent experimental results and solid lines simulation results.

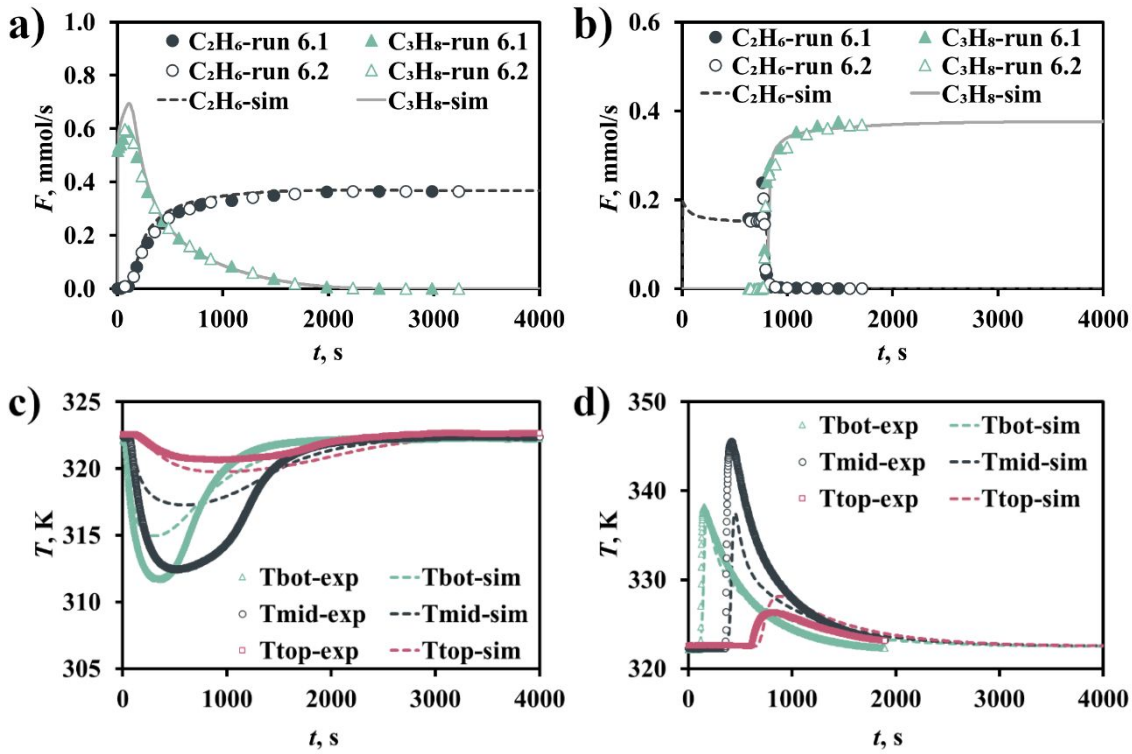

Figure S12. Molar flow rates (a) adsorption of ethane over a bed initially full of propane at 323 K and 150 kPa; (b) desorption of previously adsorbed ethane in flowing propane at 323 K and 150 kPa; gas temperature history along the (c) adsorption and (d) desorption at 0.17 m, 0.42 m and 0.67 m from the bottom end of the column. Symbols represent experimental results and solid lines simulation results.

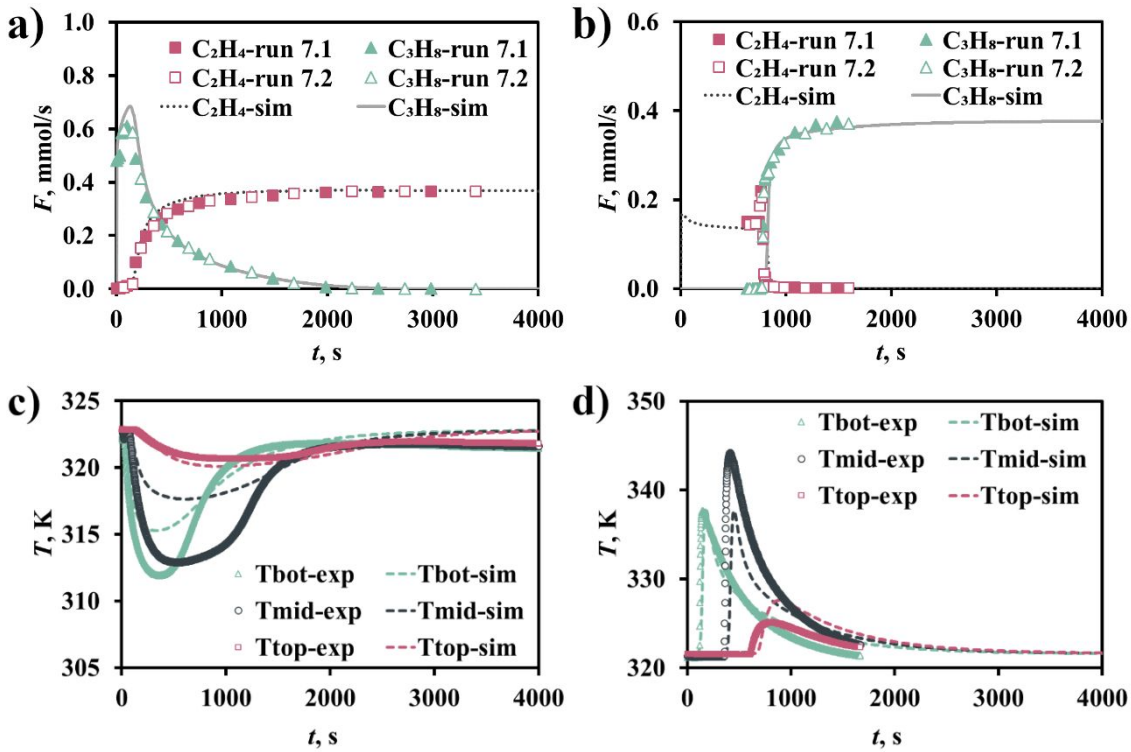

Figure S13. Molar flow rates (a) adsorption of ethylene over a bed initially full of propane at 323 K and 150 kPa; (b) desorption of previously adsorbed ethylene in flowing propane at 323 K and 150 kPa; gas temperature history along the (c) adsorption and (d) desorption at 0.17 m, 0.42 m and 0.67 m from the bottom end of the column. Symbols represent experimental results and solid lines simulation results.

VPSA Cycles

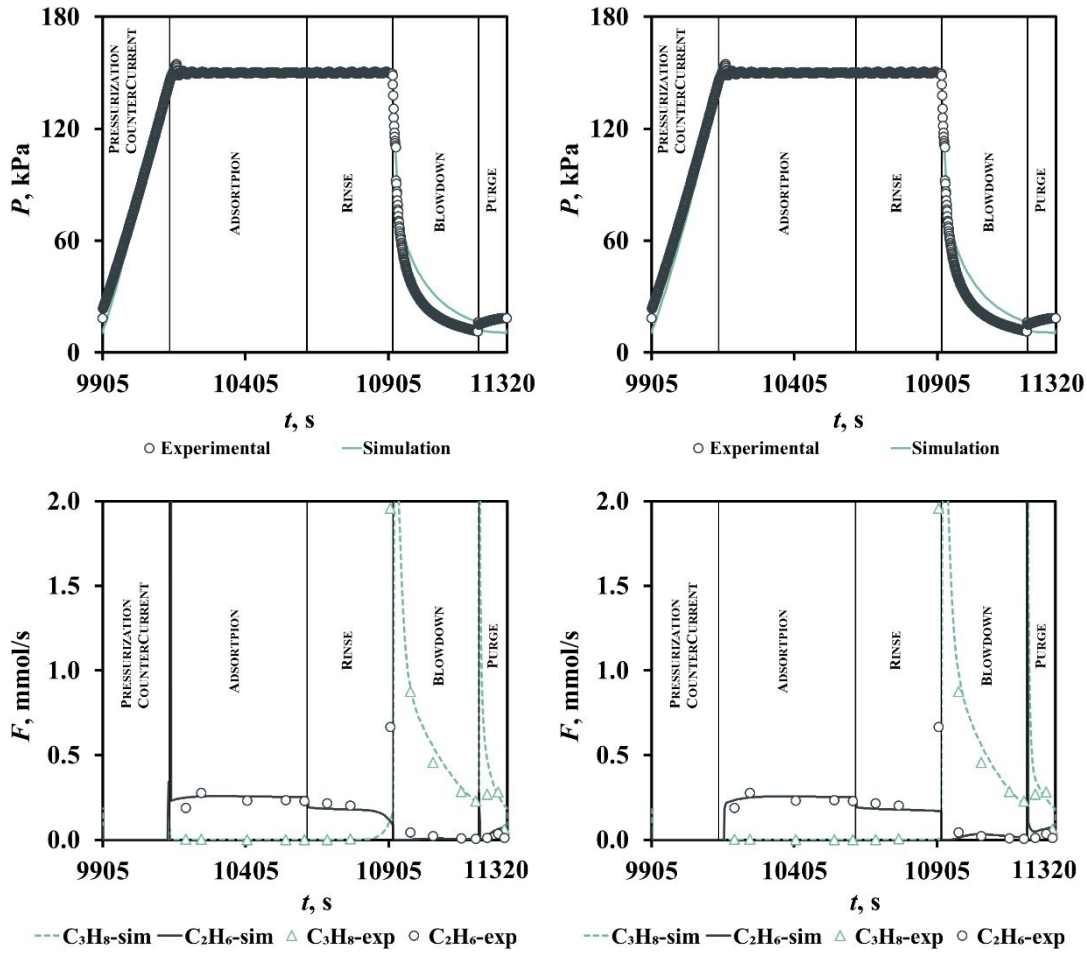

Figure S14. Last (8th) cycle performed for the VPSA scheme 1 on MIL-100(Fe) granules: pressure history; molar flow rates of ethane and propane at the column exit considering a q_{sat} of 95% (left) and a q_{sat} of 105% (right). Symbols represent the experimental results and lines the simulation results.

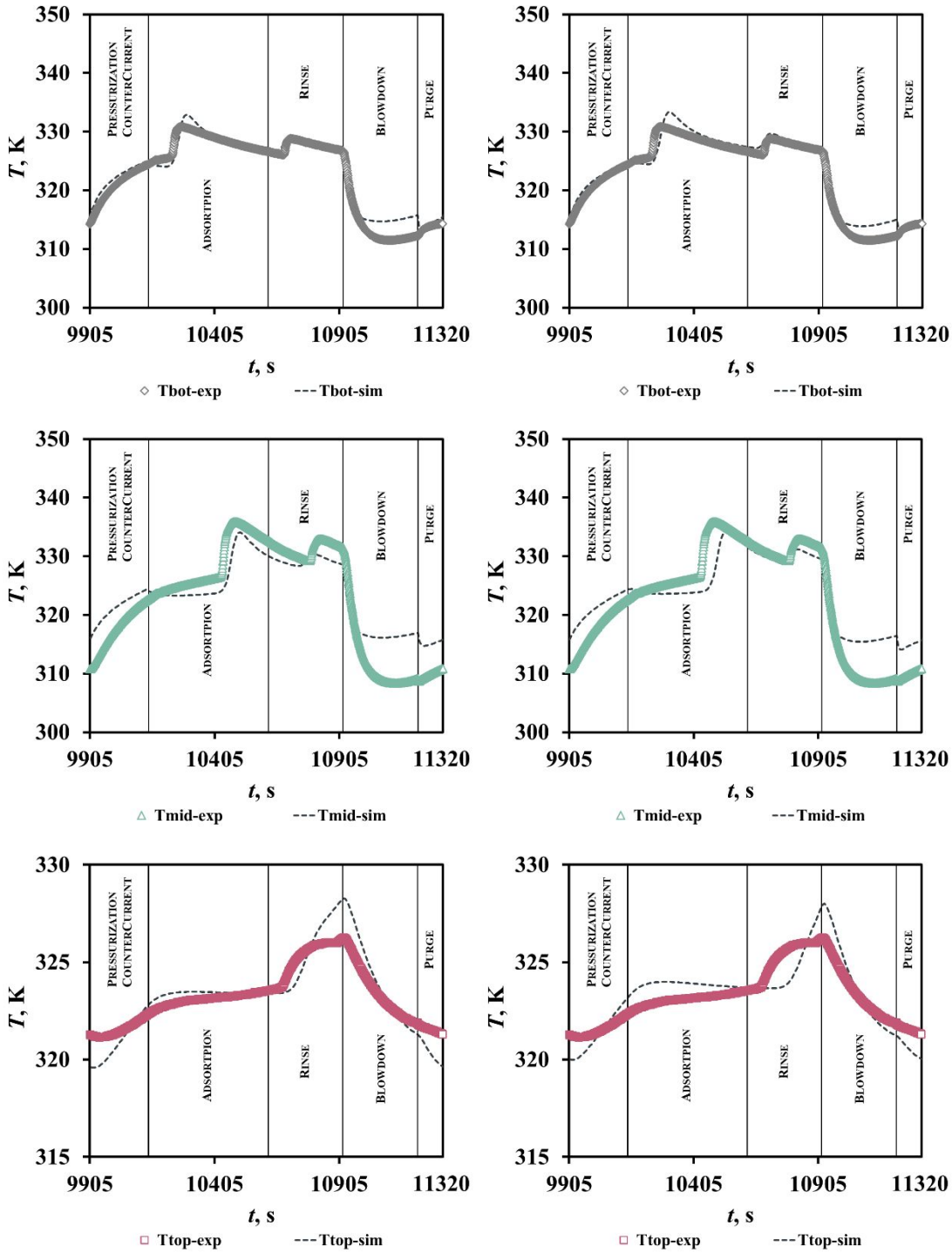

Figure S15. Last (8th) cycle performed for the VPSA scheme 1 on MIL-100(Fe) granules: gas temperature history at 0.17 m (bottom), 0.42 m (middle) from the bottom end of the column; and column wall temperature at 0.67 m (top) from the bottom end of the column considering a q_{sat} of 95% (left) and a q_{sat} of 105% (right). Symbols represent the experimental results and lines the simulation results.

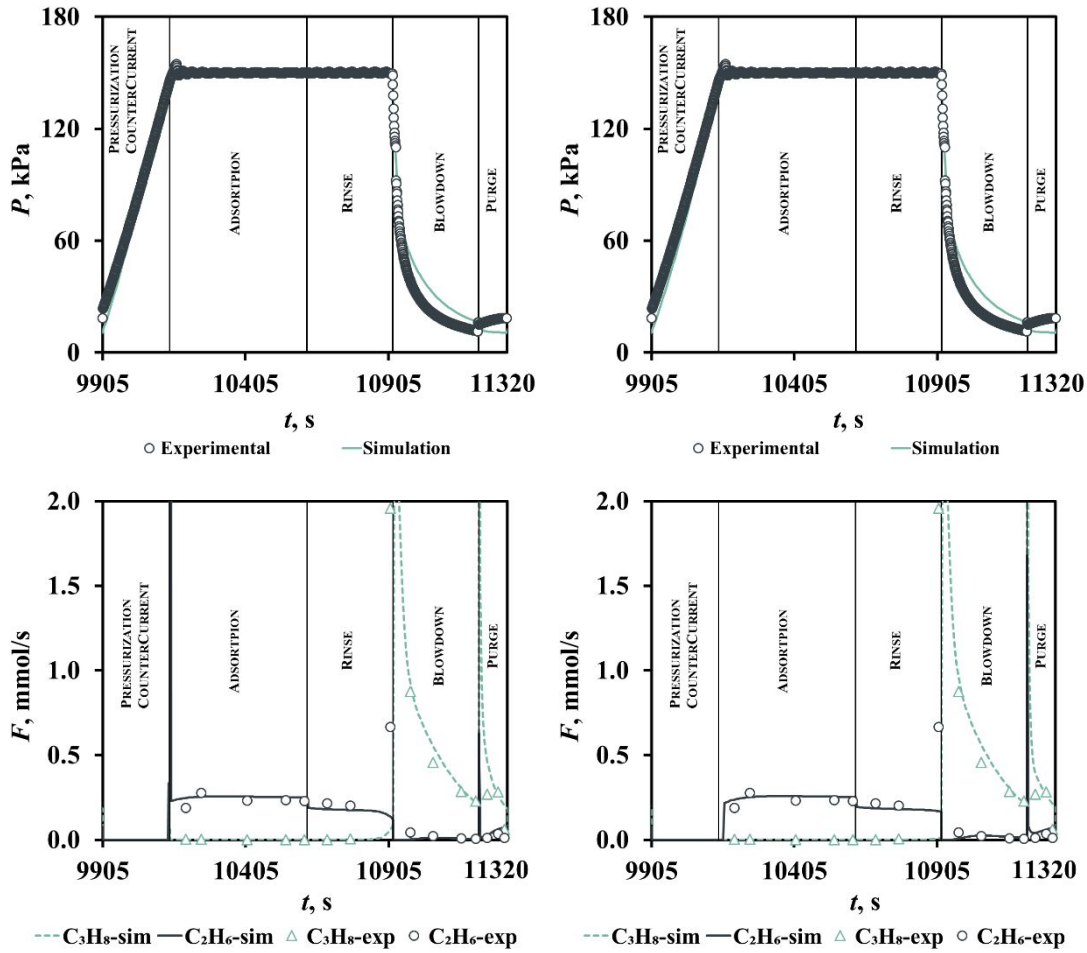

Figure S16. Last (8th) cycle performed for the VPSA scheme 1 on MIL-100(Fe) granules: pressure history; molar flow rates of ethane and propane at the column exit considering a b_∞ of 95% (left) and a b_∞ of 105% (right). Symbols represent the experimental results and lines the simulation results.

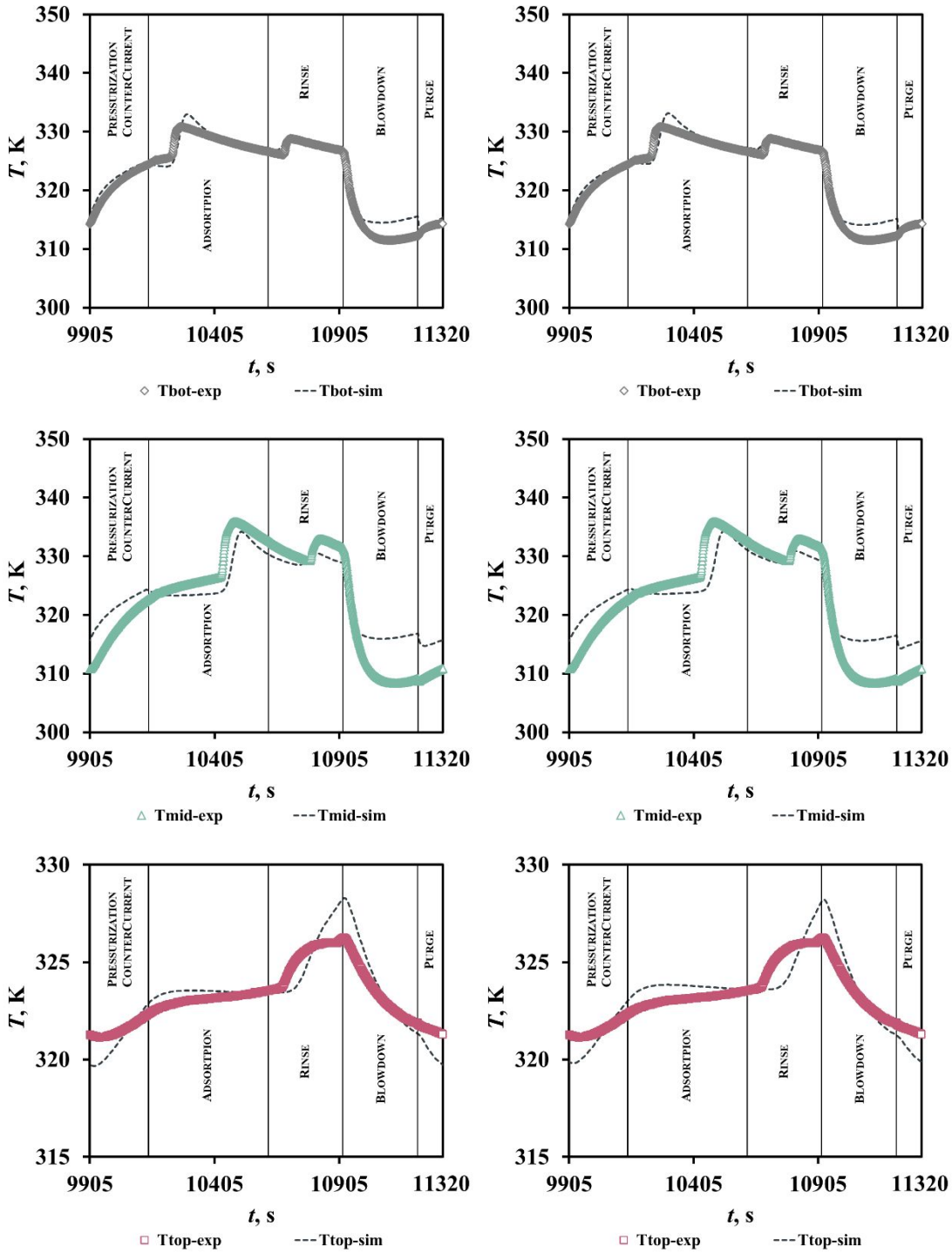

Figure S17. Last (8th) cycle performed for the VPSA scheme 1 on MIL-100(Fe) granules: gas temperature history at 0.17 m (bottom), 0.42 m (middle) from the bottom end of the column; and column wall temperature at 0.67 m (top) from the bottom end of the column considering a b_∞ of 95% (left) and a b_∞ of 105% (right). Symbols represent the experimental results and lines the simulation results.

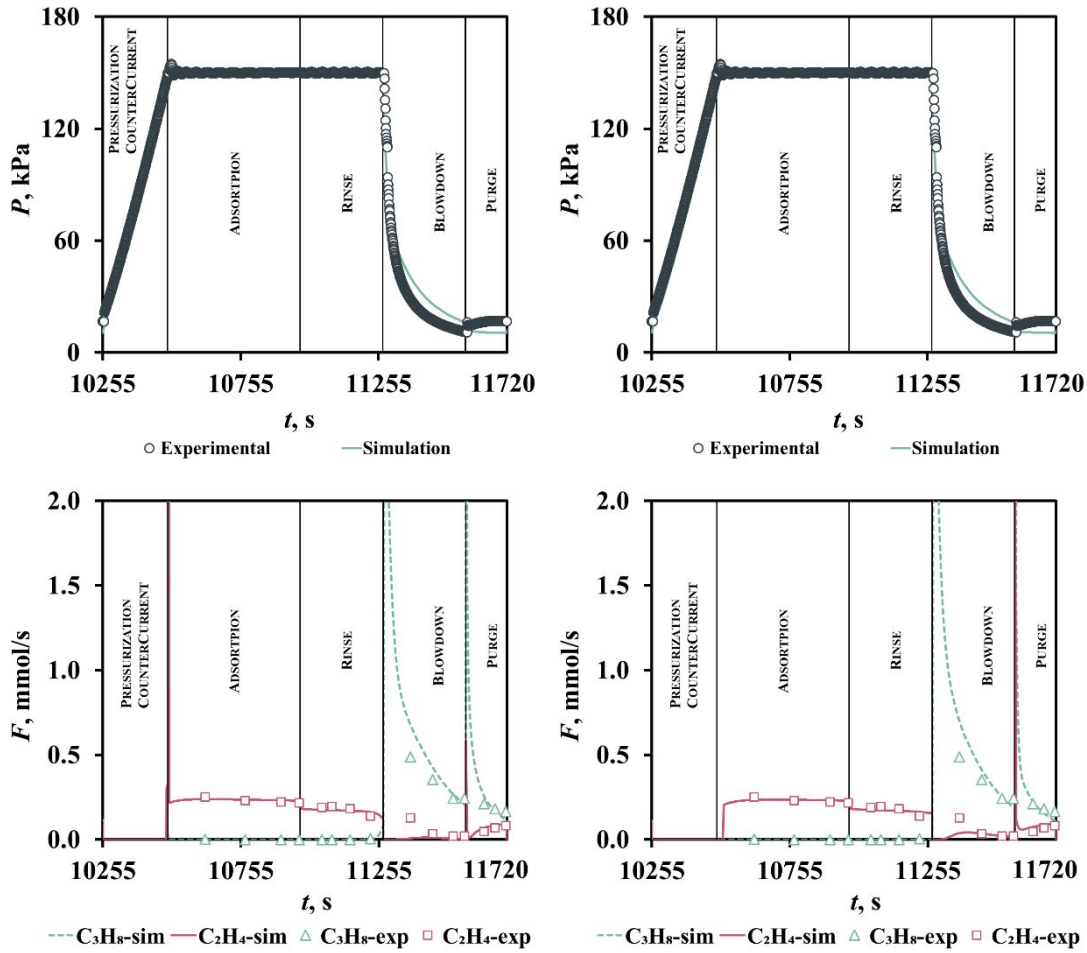

Figure S18. Last (8th) cycle performed for the VPSA scheme 2 on MIL-100(Fe) granules: pressure history; molar flow rates of ethylene and propane at the column exit considering a q_{sat} of 95% (left) and a q_{sat} of 105% (right). Symbols represent the experimental results and lines the simulation results.

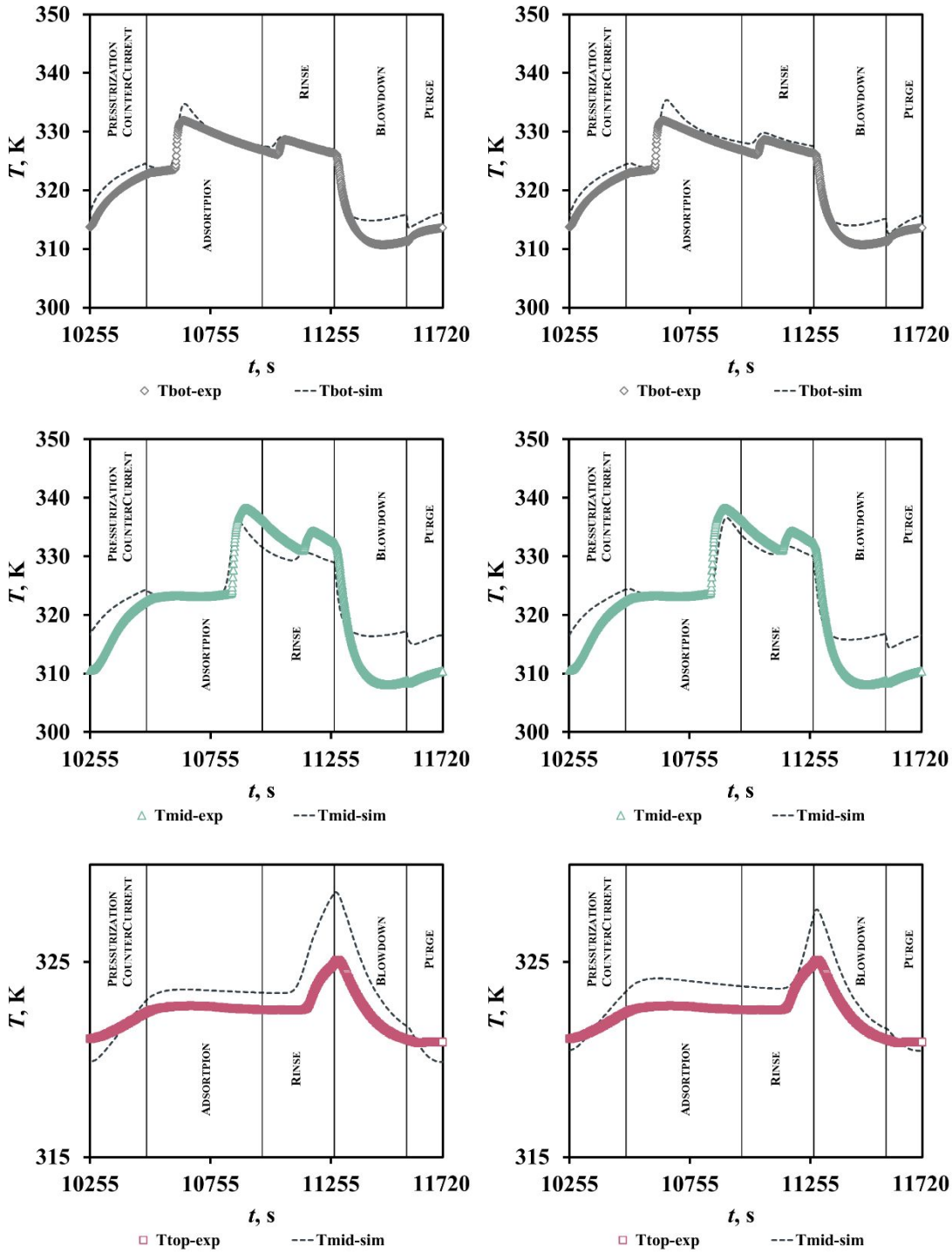

Figure S19. Last (8th) cycle performed for the VPSA scheme 2 on MIL-100(Fe) granules: gas temperature history at 0.17 m (bottom), 0.42 m (middle) from the bottom end of the column; and column wall temperature at 0.67 m (top) from the bottom end of the column considering a q_{sat} of 95% (left) and a q_{sat} of 105% (right). Symbols represent the experimental results and lines the simulation results.

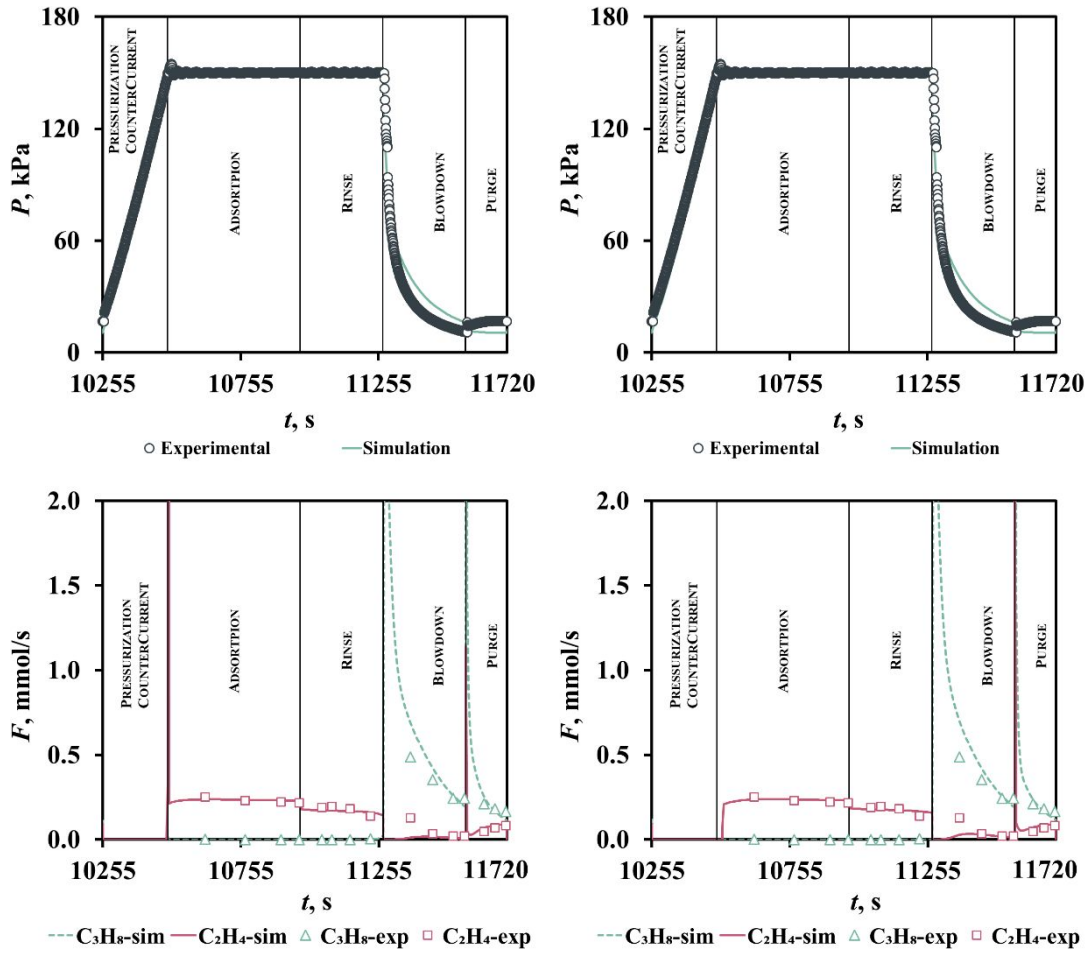

Figure S20. Last (8th) cycle performed for the VPSA scheme 2 on MIL-100(Fe) granules: pressure history; molar flow rates of ethylene and propane at the column exit considering a b_∞ of 95% (left) and a b_∞ of 105% (right). Symbols represent the experimental results and lines the simulation results.

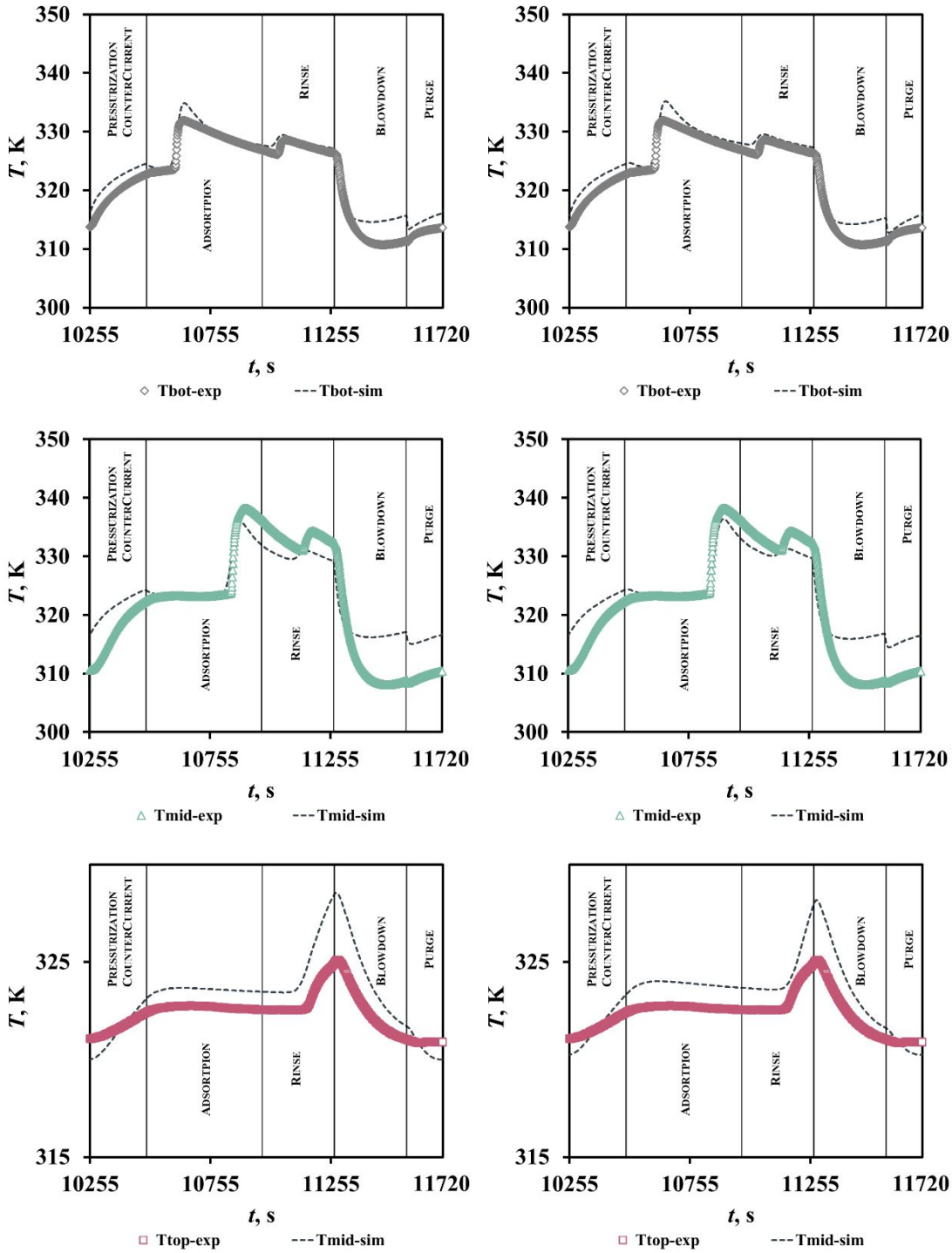

Figure S21. Last (8th) cycle performed for the VPSA scheme 2 on MIL-100(Fe) granules: gas temperature history at 0.17 m (bottom), 0.42 m (middle) from the bottom end of the column; and column wall temperature at 0.67 m (top) from the bottom end of the column considering a b_∞ of 95% (left) and a b_∞ of 105% (right). Symbols represent the experimental results and lines the simulation results.

RAW DATA

Equilibrium isotherms data:

P (kPa)	q (mol/kg)
24.490	0.206
61.340	0.519
204.210	1.523
403.550	2.609
816.600	4.100
597.790	3.403
95.980	0.825

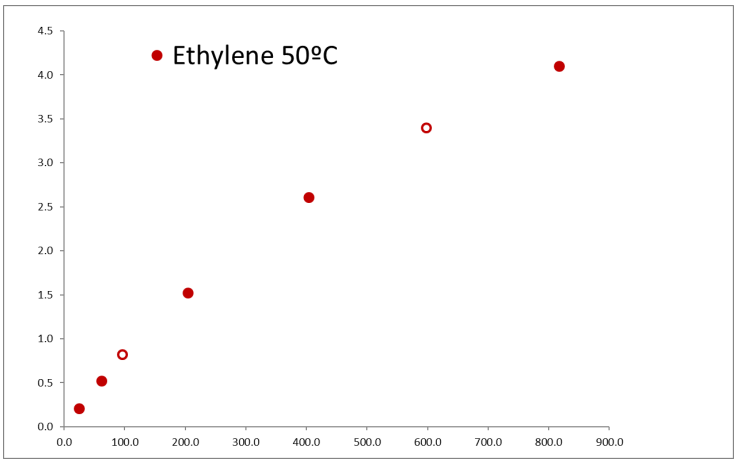

P (kPa)	q (mol/kg)
18.820	0.084
49.580	0.208
195.800	0.660
402.460	1.228
790.700	2.267
590.510	1.705
95.600	0.433

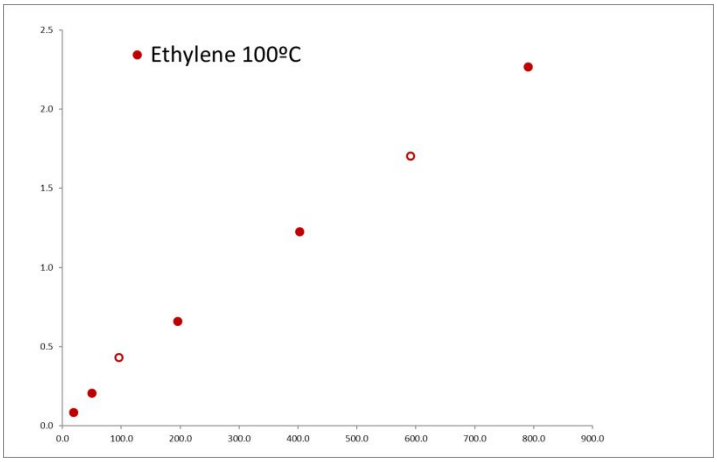

P (kPa)	q (mol/kg)
13.070	0.022
52.330	0.097
198.820	0.355
399.200	0.674
790.570	1.448
598.260	0.976
98.150	0.220

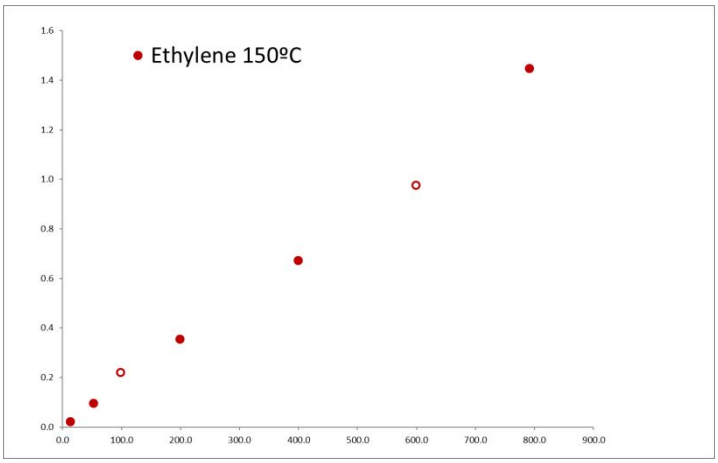

P (kPa)	q (mol/kg)
13.066	0.126
52.850	0.540
192.660	1.750
394.920	3.075
780.600	4.659
568.980	3.956
106.900	1.051

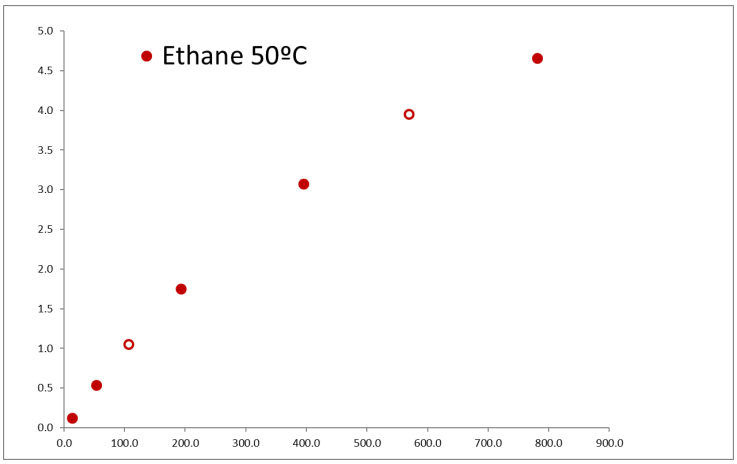

P (kPa)	q (mol/kg)
12.970	0.056
48.504	0.180
201.254	0.673
410.925	1.302
792.120	2.257
598.580	1.815
97.679	0.380

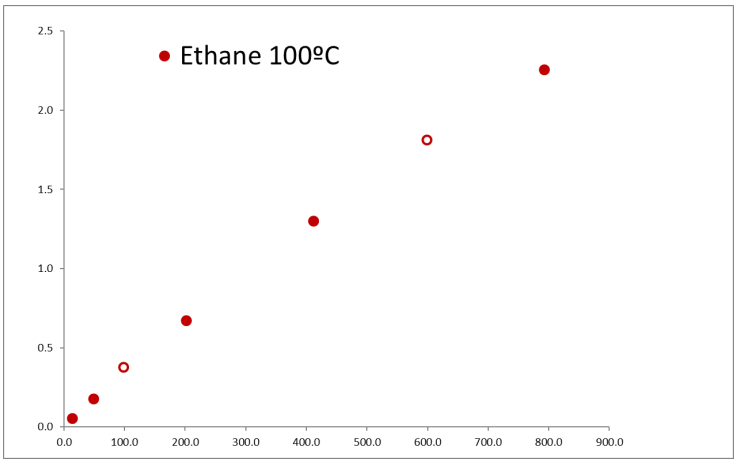

P (kPa)	q (mol/kg)
12.990	0.043
48.113	0.104
197.018	0.344
399.126	0.654
797.123	1.175
593.570	0.929
98.336	0.207

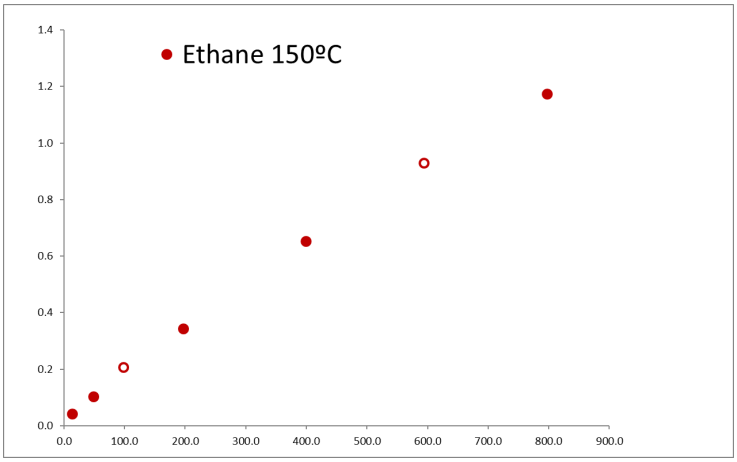

P (kPa)	q (mol/kg)
9.952	0.427
93.673	3.198
193.772	4.437
393.512	5.550
784.991	6.226
594.553	6.030
67.482	2.621

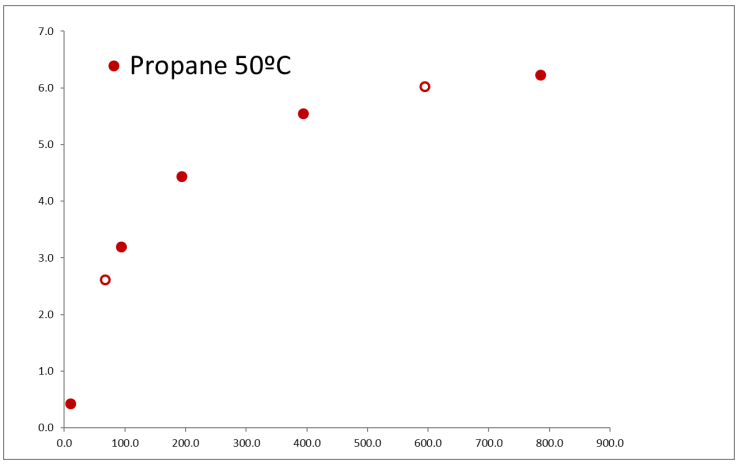

P (kPa)	q (mol/kg)
22.825	0.269
47.098	0.539
194.755	1.939
398.031	3.351
794.000	4.856
590.614	4.216
110.268	1.204

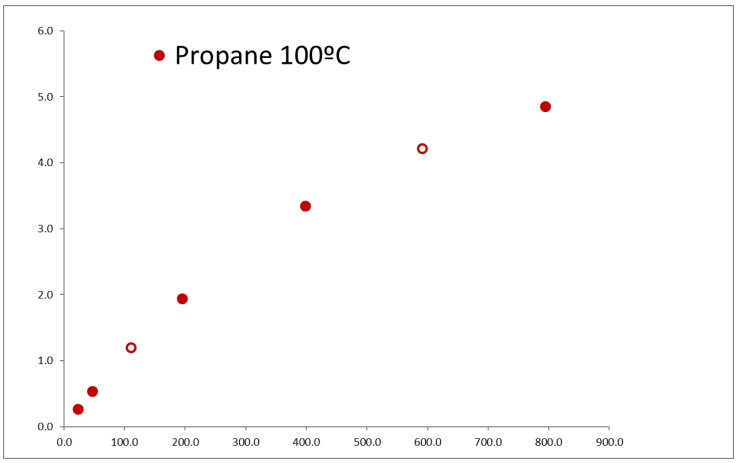

P (kPa)	q (mol/kg)
12.979	0.076
55.228	0.240
204.500	0.812
401.787	1.695
799.000	3.229
598.944	2.528
105.847	0.452

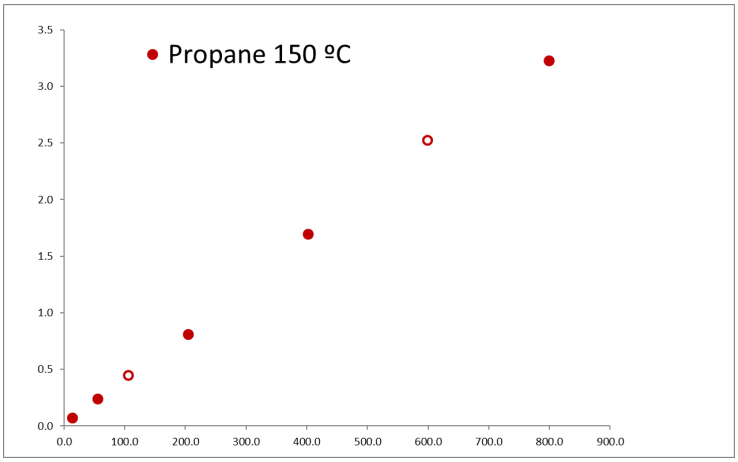

Breakthrough experiments data:

Single ethane:

Time, s	yethane
214	0.003099134
297	0.000737907
303	0.004874727
310	0.086964795
322	0.729318067
329	0.91081837
334	0.948244745
344	0.955749918
379	0.969921986
399	0.987930406
429	0.975798294
461	0.971325268
579	0.990250693
759	0.983873482
960	0.992426226
3429	1
3608	1
3759	1

Time, s	yethane
5	0.916484988
13	1.039142268
21	1.023301724
28	0.918192418
37	0.865185472
48	0.807590974
78	0.670590722
125	0.594946233
178	0.463737102
278	0.286146882
451	0.075227019
698	0.032148152
999	0.010539791
1398	0.005685132
2001	0.003388899

Time, s	yethane
243	0.005545429
299	0.001690645
304	0.002547403
310	0.022717073
315	0.280654939
320	0.665559466
325	0.84751748
330	0.93655201
335	0.942607941
340	0.961267834
373	1.006102016
448	0.981459297
597	0.942211118
763	1.00967682
1057	1.006703142
4258	1.001467285
4402	1.005309436
4547	1.015607402

Time, s	yethane
3	0.836500203
14	1.068182168
23	1.004894699
59	0.812816382
89	0.662516439
151	0.521673783
242	0.357099207
349	0.193522273
598	0.053887656
899	0.0143904
1149	0.007234672
1699	0.003821829
2198	0.002475319
2498	0.001955562
2811	0.001715846

Single ethylene:

Time, s	yethylene
18	0.0055
48	0.000764305
64	0.000798207
83	0.003551028
113	0.001417989
143	0.000932155
173	0.001041249
223	0.003077968
273	0.044847055
323	0.785142352
423	0.972115303
483	0.978341605
583	0.985401354
704	0.962832397
883	0.982176367
3575	1
3838	1
4126	1

Time, s	yethylene
15	0.772312473
25	1.014832575
39	0.88890327
60	0.760137853
86	0.648285636
120	0.537624527
180	0.424031755
280	0.274526284
359	0.156081023
450	0.109222695
700	0.040153869
999	0.015701585
1400	0.008257856
1949	0.004001621

Time, s	yethylene
259	0.0041
274	0.001313977
284	0.003808557
294	0.04132217
304	0.727330923
314	0.926290886
324	0.980663546
333	0.982532299
344	0.9843169
359	0.989639006
370	1.019642706
390	1.001709975
404	1.011375525
420	0.993230742
819	1.012190682

Single propane:

Time, s	ypropane
198	0.001501592
723	0.000434279
733	0.001428521
743	0.020727742
754	0.477235065
764	0.820293404
778	0.925909947
794	0.91489762
808	0.944014396
838	0.948333362
868	1.005069592
918	0.951247203
1019	0.991180821
1218	0.97834973
1521	0.996419077
4078	1
4269	1
4893	1

Time, s	ypropane
5	0.91632793
19	1.031187564
39	0.878585879
61	0.772836817
78	0.717801303
110	0.660887234
129	0.62282029
179	0.580698181
275	0.511784626
359	0.465191568
481	0.406555485
769	0.348759068
1080	0.261156551
1399	0.187438824
2105	0.042194214

Time, s	ypropane
704	0.003139417
742	0.000998471
747	0.002171943
752	0.001731095
757	0.009236173
762	0.145603057
767	0.56611247
772	0.833365652
777	0.899871326
797	0.953323985
829	0.953653826
889	0.956571383
991	0.980843174
1213	0.9911798
4390	1.008107685
4588	0.983815726
4818	1.008076589

Time, s	ypropane
2	0.856254861
8	1.051903405
28	0.931681556
87	0.726430347
221	0.568211439
318	0.485257673
447	0.428889766
597	0.384720637
748	0.346461501
870	0.301349857
1200	0.234004658
1610	0.14191155
1800	0.078058474
2402	0.01880579
2901	0.004796531

Binary 30ethane/70propane vs Helium:

Time, s	yethane	ypropane
456	0.002675114	0.001793
510	0.000405386	0.000205
514	0.000524228	0.000231
520	0.001949643	0.000807
525	0.00147662	0.000234
530	0.00289334	0.000185
535	0.03258732	0.000148
544	0.624096313	0.00022
559	0.905925871	0.000505
589	0.981281654	0.000656
639	1.006834224	0.003112
749	0.9563	0.0437
889	0.4863	0.5137
1024	0.3619	0.6381
1248	0.3207	0.6793
4888	0.2776	0.7224
5088	0.2810	0.7190
5289	0.2797	0.7203

Time, s	yethane	ypropane
4	0.255670483	0.659663
9	0.303187595	0.770442
19	0.298687087	0.747127
34	0.237054535	0.664256
50	0.200195451	0.616201
89	0.150927064	0.551575
124	0.108727158	0.509972
322	0.015842429	0.451128
449	0.004966499	0.400926
699	0.002617031	0.328803
999	0.001859835	0.274825
1299	0.001444011	0.201603
1599	0.001337138	0.119811
2535	0.000772001	0.022222

Time, s	yethane	ypropane
446	0.002444882	0.001497
512	0.000906352	0.000991
531	0.001482447	0.000807
537	0.007349995	0.001688
541	0.080793865	0.00103
548	0.67606277	0.00102
701	0.9992	0.0008
767	0.9991	0.0009
793	0.9977	0.0023
838	0.9657	0.0343
868	0.5456	0.4544
961	0.3897	0.6103
1148	0.3319	0.6681
1148	0.3021	0.6979
1755	0.2940	0.7060
5018	0.2778	0.7222
5246	0.2779	0.7221
5446	0.2684	0.7316

Time, s	ethane	propane
14	0.240495189	0.643614
25	0.282284572	0.752841
39	0.237196079	0.679883
69	0.171486248	0.596342
99	0.129233137	0.541948
209	0.058625886	0.477794
249	0.029328803	0.453171
380	0.007877429	0.432265
599	0.003317798	0.376809
870	0.001435653	0.300041
1174	0.001560969	0.224297
1399	0.001101347	0.171698
1799	0.00110213	0.074489
2464	0.000869129	0.01641
2950	0.000703188	0.003763

Time, s	yethane	ypropane
544	0.010847929	0.001403
556	0.723226581	0.000588
650	0.9995	0.0005
670	0.9990	0.0010
690	0.9994	0.0006
710	0.9995	0.0005
730	0.9995	0.0005
750	0.9994	0.0006
770	0.9992	0.0008
790	0.9991	0.0009
810	0.9980	0.0020
830	0.9965	0.0035
850	0.9697	0.0303
870	0.5989	0.4011
1080	0.3554	0.6446

Binary 30ethylene/70propane vs Helium:

Time, s	yethylene	ypropane
448	0.002578408	0.000465
517	0.000448131	0.000281
537	0.029462687	0.000401
548	0.730824985	0.001768
558	0.907301052	0.001398
578	0.958437856	0.001426
647	0.984870889	0.002637
747	1.003020792	0.001512
828	0.9981	0.0019
848	0.9996	0.0004
857	0.9971	0.0029
867	0.9544	0.0456
888	0.5575	0.4425
948	0.4171	0.5829
1047	0.3711	0.6289
4348	0.2976	0.7024
4357	0.2995	0.7005
4367	0.2990	0.7010

Time, s	yethane	ypropane
8	0.247699519	0.635676
18	0.309262105	0.787844
28	0.26304086	0.709722
48	0.205147275	0.633137
73	0.162001191	0.582974
98	0.126978935	0.542086
148	0.087876098	0.499983
249	0.04729325	0.462265
448	0.018086965	0.410915
698	0.006365823	0.341727
1111	0.002838056	0.244313
1508	0.001944434	0.153249
2008	0.001544909	0.037835
2508	0.001231796	0.008342
3008	0.000955565	0.002878

Time, s	yethylene	ypropane
499	0.019577722	0.001645
543	0.733386557	0.001448
559	0.897359377	0.001983
619	0.958154744	0.003588
699	0.997374761	0.002625
789	0.989231413	0.010769
868	0.689888929	0.310111
874	0.526894655	0.473105
884	0.4521	0.5479
998	0.3804	0.6196
1099	0.3536	0.6464
1198	0.3385	0.6615
1299	0.3280	0.6720
1398	0.3212	0.6788
1499	0.3161	0.6839

Time, s	yethylene	ypropane
4	0.24829889	0.646963
9	0.298254651	0.782026
24	0.275276455	0.727839
35	0.232287396	0.666019
54	0.19027833	0.615423
79	0.148584083	0.565928
124	0.104506957	0.516565
199	0.062962379	0.47977
389	0.027686068	0.432088
550	0.010383511	0.375467
899	0.003936398	0.290991
1299	0.002237401	0.204792
1749	0.001580929	0.088809
2249	0.001392683	0.019855
2800	0.001055269	0.004485

Pseudo-binary ethane vs propane:

Time, s	yethane	ypropane
4	0.005372423	0.994628
9	0.001204587	0.998795
29	0.00153667	0.998463
69	0.007150661	0.992849
119	0.015172255	0.984828
199	0.142616342	0.857384
299	0.322432749	0.677567
449	0.490504057	0.509496
598	0.602476375	0.397524
799	0.701106081	0.298894
1099	0.798841623	0.201158
1498	0.9021	0.0979
1998	0.9811	0.0189
2498	0.9954	0.0046
2998	0.9979	0.0021

Time, s	yethane	ypropane
649	0.997801505	0.002198
699	0.998948659	0.001051
718	0.998614108	0.001386
738	0.99755522	0.002445
748	0.998503697	0.001496
761	0.998220247	0.00178
778	0.987812994	0.012187
798	0.653612846	0.346387
819	0.115704746	0.884295
838	0.028001954	0.971998
858	0.016039747	0.98396
949	0.009027367	0.990973
1099	0.005367171	0.994633
1298	0.003304445	0.996696
1498	0.002557872	0.997442

Time, s	yethane	ypropane
7	0.005307903	0.994692
19	0.001210822	0.998789
49	0.002213584	0.997786
89	0.014349946	0.98565
169	0.075956539	0.924043
249	0.242433432	0.757567
369	0.410371508	0.589628
499	0.537023986	0.462976
700	0.650227609	0.349772
898	0.741264783	0.258735
1299	0.850576922	0.149423
1700	0.9442	0.0558
2249	0.9896	0.0104
2749	0.9966	0.0034
3249	0.9982	0.0018

Time, s	yethane	ypropane
668	0.997503534	0.002496
728	0.9989364	0.001064
748	0.998491786	0.001508
768	0.996866744	0.003133
778	0.997499924	0.0025
788	0.987201645	0.012798
798	0.671011803	0.328988
808	0.190768937	0.809231
848	0.040673338	0.959327
899	0.013382558	0.986617
1013	0.007398826	0.992601
1198	0.004510324	0.99549
1399	0.002878715	0.997121
1604	0.002232301	0.997768
1722	0.002028135	0.997972

Pseudo-binary ethylene vs propane:

Time, s	yethylene	ypropane
4	0.006781829	0.993218
9	0.001174143	0.998826
28	0.001486582	0.998513
68	0.007623393	0.992377
118	0.018576719	0.981423
198	0.170522319	0.829478
298	0.365679432	0.634321
448	0.522613644	0.477386
598	0.6220819	0.377918
798	0.710929237	0.289071
1098	0.79782639	0.202174
1498	0.8970	0.1030
1998	0.9802	0.0198
2498	0.9959	0.0041
2998	0.9982	0.0018

Time, s	yethylene	ypropane
648	0.9983	0.0017
698	0.9989	0.0011
718	0.9991	0.0009
738	0.9981	0.0019
748	0.9986	0.0014
758	0.9984	0.0016
778	0.9869	0.0131
799	0.4367	0.5633
818	0.0954	0.9046
838	0.0293	0.9707
870	0.0159	0.9841
949	0.0096	0.9904
1099	0.0065	0.9935
1298	0.0041	0.9959
1498	0.0032	0.9968

Time, s	yethylene	ypropane
14	0.006937406	0.993063
19	0.001309536	0.99869
48	0.00191243	0.998088
88	0.01056759	0.989432
168	0.032375539	0.967624
248	0.271218872	0.728781
368	0.449714564	0.550285
499	0.565354188	0.434646
699	0.664719779	0.33528
899	0.746433717	0.253566
1299	0.846369407	0.153631
1698	0.9397	0.0603
2249	0.9893	0.0107
2749	0.9973	0.0027
3422	0.9985	0.0015

Time, s	yethylene	ypropane
668	0.997578577	0.002421
729	0.999016476	0.000984
769	0.998437194	0.001563
789	0.983543971	0.016456
799	0.499433028	0.500567
809	0.132040859	0.867959
819	0.051647661	0.948352
829	0.03016535	0.969835
839	0.0219205	0.978079
849	0.017998479	0.982002
899	0.012812271	0.987188
999	0.007952156	0.992048
1198	0.005121752	0.994878
1399	0.003230761	0.996769
1610	0.002593632	0.997406

References

1. Mofarahi M., Salehi S.M. Pure and binary adsorption isotherms of ethylene and ethane on zeolite 5A. *Adsorption*. 2013;19:101-110.

2. Narin G., Martins V.F.D., Campo M., Ribeiro A.M., Ferreira A., Santos J.C., Schumann K., Rodrigues A.E. Light olefins/paraffins separation with 13X zeolite binderless beads. *Sep Purif Technol*. 2014;133:452-475.

3. Shi M., Avila A.M., Yang F., Kuznicki T.M., Kuznicki S.M. High pressure adsorptive separation of ethylene and ethane on Na-ETS-10. *Chem Eng Sci*. 2011;66:2817-2822.

4. Fatemi S., Masoudi-Nejad M. Application of Zeotype SAPO-34 Molecular Sieve as a Selective Adsorbent for Separation of Ethylene from Ethane. *Gas Processing*. 2014;2:1-7.

5. Poling B., Prausnitz J., Connell J.O. *The Properties of Gases and Liquids*: McGraw-Hill Education; 2000.

6. Bird R.B., Stewart W.E., Lightfoot E.N. *Transport Phenomena*: Wiley; 2007.